

## Synthesis and Characterization of Sweet Potato Starch Biocomposite Incorporated with ZnO Nanoparticles

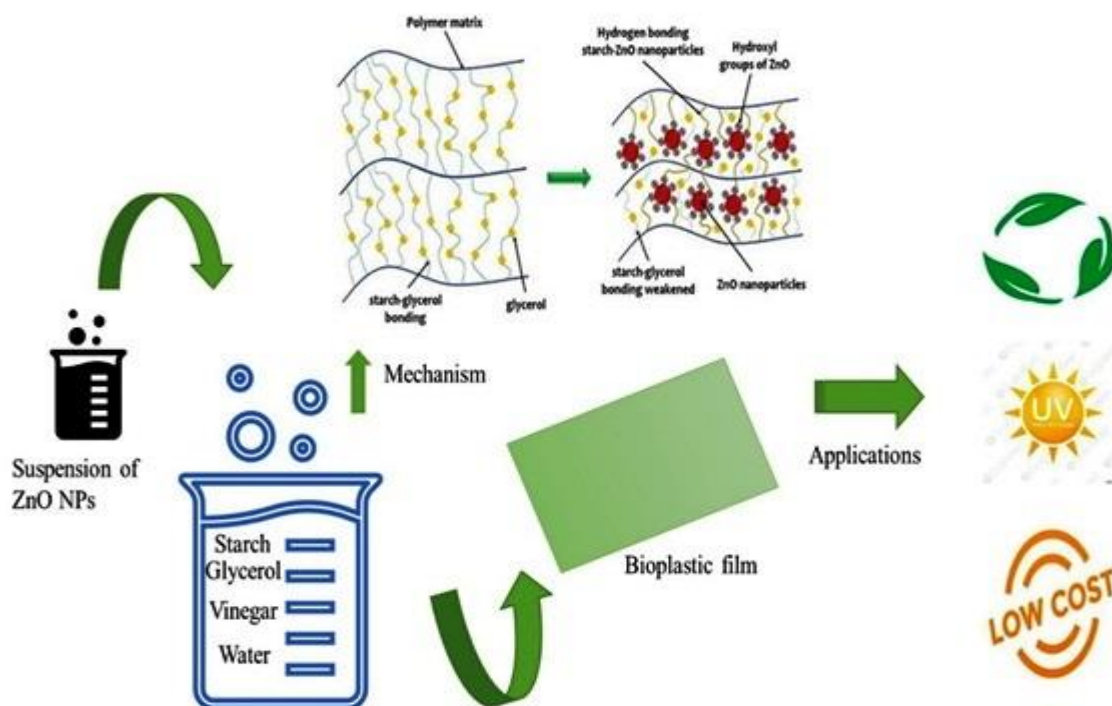
<sup>1</sup>Saira Iqbal\*, <sup>2</sup>Arjumand Iqbal Durrani and <sup>2</sup>Ashi Rashid

<sup>1,2</sup>Department of Chemistry, University of Engineering and Technology Lahore, Pakistan.  
Sairaiqbal900@gmail.com\*

(Received on 07<sup>th</sup> December 2021, accepted in revised form 19<sup>th</sup> December 2022)

**Summary:** The rapid rise in the production of hazardous waste in the environment, particularly single-use plastics, has prompted the development of sustainable yet cost-effective alternatives. This research aims to create bioplastic films using renewable energy sources. To prevent toxic side products, the composite bioplastics synthesized from sweet potato starch are incorporated with biogenically synthesized ZnO NPs. Biocomposite films were characterized by their morphology, water vapor permeability (WVP), biodegradability, thermal and mechanical properties. It was noted that the ZnO NPs had substantial effects on the tensile properties of the nanocomposite films. The addition of ZnO NPs to the starch bioplastic films considerably enhanced tensile strength from 1.41 to 2.26 MPa, elongation from 78.20 to 114.91%, and Young's modulus from 1.62 to 2.40 MPa. The incorporation of ZnO NPs lowered the degree of WVP and film solubility value compared to those of the starch films. The bioplastic film incorporated with ZnO NPs had effective UV absorption and transparency. The shift in the peaks in the FT-IR spectra confirmed the relationship between the polymer matrix and the ZnO NPs. Thermal degradation of bio nanocomposite at 339.60 °C is shown by a consistent reduction in TGA between 240 °C and 410 °C. The high melting temperature ( $T_m$ ) of 144 °C for starch film and 201.86 °C for bio nanocomposite was found using DSC analysis. SEM analysis revealed that biocomposite films had better compatible morphologies with small cracks and the roughness of films increased with the addition of ZnO NPs content. The biodegradability of the biocomposite films was analyzed through the soil burial method. The bioplastic produced in this study has the potential to be a viable alternative to existing conventional plastics in the packaging industry.

### Graphical abstract



**Keywords:** Biodegradable; Bioplastic; Biopolymer; Nanocomposite; Nanoparticles.

\*To whom all correspondence should be addressed.

## Introduction

Petroleum-based plastic materials are being used in an extensive variety of applications owing to their valuable properties. A significant amount of the plastics at present have been produced from conventional petroleum-based substances and therefore not prepared from natural sources [1]. Global plastics manufacture and consumption have been growing each year and consequently is a rising concern about its influence on the surroundings due to the incapability of conventional petroleum-based plastic materials to decompose which is also condemned by environmental scientists [2]. The disposal of these materials into the environment may lead to severe consequences due to their low biodegradability. Hence, extensive research is being done and underway to develop new biodegradable biocomposites from renewable resources [3]. Compostable plastic materials are prepared from cellulose, starch, chitosan, and protein obtained from sustainable resources.

New methods have been investigated resulting in a significant reduction in both energy consumption (as much as 60 %) and conservatory gases compared to methods used for the production of traditional plastic materials [4]. Bioplastics are currently being used as disposable materials and the effect of diverse environmental conditions has been studied on the degradation of these bioplastics [5]. For this purpose, primarily starch bioplastic composites are being explored for developing sustainable materials because of their renewability, cheap and exceptional biodegradable properties [6, 7] but many of the studied starch-based polymers exhibited low thermal and mechanical stability [8,9,10]. Plastic manufactured by use of bio-based starch from selected starch-rich roots has also been analyzed and evaluated for its stability and biodegradable properties [11]. This type of bio-based plastic material has demonstrated better physio-mechanical and thermal properties with great decomposability that marks them an appropriate substitute for the prevailing traditional plastic [6]. In the laboratory, bioplastics based on sweet potato starch (*Ipomoea batatas*) have also been prepared for being cost-effective and biocompatible [12].

The use of additives such as nano-sized fillers and bio cross-linkers has been investigated to improve the lifespan, viscoelasticity, conductivity, and thermal characteristics of the bioplastic nanocomposite [13]. Moreover, a comparatively compact, and integrated structure is achieved by the addition of the glycerol plasticizer to starch bioplastic due to the packing of the vacant spaces between starch polymer chains. The

plasticized starch composite blended with various bio fillers has been shown to improve the physical characteristics by various physical and chemical modifications [14]. Composite materials containing NPs and glycerol as a plasticizer have proven themselves as high-performance advanced materials with exceptional interfacial interactions [15].

The properties of Nano-fillers persuade the durable inter-facial connection between Nano-fillers and polymer medium that develops the polymer characteristics. ZnO NPs have been drawing excessive attention as a multipurpose Nano-filler [16] due to their antimicrobial action and demanding UV captivation. Green synthesis of ZnO NPs using guava leaves has been described to be effective due to its enhanced antibacterial characteristics [17]. Different fragments of neem trees such as stems, leaves, and fruits have also been studied for the synthesis of ZnO NPs. Biological techniques have been proven as an appropriate route to produce ZnO NPs in a well-ordered and accurate way.

Numerous investigators have examined the strengthening of polymeric mixtures by using ZnO for food packaging [18, 19]. Dynamic packing has been developed to prolong food shelf life and preserve food quality. Instead of exploring unconventional ways to reduce the global demand for plastic, another way is to increase the efficiency more sustainably by manufacturing bioplastics that showed maximum degradation and had no effect on bacterial diversity and Nitrogen circulation activity[20]. Oleyaei et al. [21] developed starch films by assimilating TiO<sub>2</sub> NPs into the potato starch polymer substance. Kanmani and Rhim [22] fabricated bio-nanocomposite films through solvent casting techniques based on different biopolymers (agar, carrageenan, or CMC) reinforced with ZnO NPs. Sanuja et al. [7] and Jayasuriya et al. [23] prepared chitosan based bio-nanocomposites by integrating ZnO NPs.

As starch is the main component (85% of the dry matter) of sweet potato root tuber, Hence, the consumption and development of sweet potato starch improved considerably owing to its fundamental characteristics [24]. Some properties like cost-effectiveness and transparent grains make it a suitable polymer for the production of bio-nanocomposite [25].

Nowadays, medicinal plants-based nanomaterials such as biogenic nanoparticles have the primary portion in green medicine and nanotechnology. The development of reliable and eco-friendly processes for the synthesis of nanoparticles is a significant step for the introduction of applications

of nanotechnology into biocomposite research. Environmentally safe biosynthesis of ZnO NPs using plant water extracts leads to the novelty and enhancement in the formation and characteristics of biocomposite materials [26,27].

Therefore, numerous researchers have investigated a range of biocomposites prepared from biogenically synthesized metal nanoparticles exhibiting enhanced properties, however, the use of ZnO NPs presents a novel approach to the synthesis of bioplastic materials. Therefore, this research work investigates the synthesis and characterization of thermal and biodegradable properties of sweet potato starch-based bioplastic composite reinforced with ZnO NPs. The study also aims to produce novel and safe ZnO NPs to be used as nanofillers in the polymer matrix with antimicrobial properties leading to the improved resultant biodegradable plastic films. Biodegradability has been the new demand for composite bioplastics due to the rigorous accumulation of plastic waste in the marine environment causing solid waste pollution affecting the living organisms.

The novel approach of using NPs synthesized from green methods for the fabrication of biocomposites offers biodegradable characteristics for use in various applications. Consequently, the fabrication of bioplastic composite films proceeded by incorporating the different amounts of ZnO NPs i.e., 1%, 3%, 5%, 7%, and 10% in a certain amount of sweet potato starch followed by inspection of their thermal stability, UV-absorbance, and soil-biodegradability properties are done in this research work.

## Experimental

### Collection of Material

Sweet Potato starch was collected from a local market in Lahore and its roots were washed, skinned, and sliced for starch extraction according to the method mentioned in the literature [28]. Zn (NO<sub>3</sub>)<sub>2</sub>.6H<sub>2</sub>O, NaOH, Deionized water, Glycerol, Vinegar, and Ethanol used in this study were obtained from Sigma Aldrich and are of analytical grade.

### Preparation of ZnO NPs

Figure 1. shows the schematic representation of the synthesis of ZnO NPs using leaf extracts of *Psidium guajava* (guava) and *Azadirachta indica* (Neem) as reducing agents and zinc nitrate hexahydrate as a precursor salt according to the

procedure mentioned in the literature [29]. For the preparation of 10% leaf extract, 10 g of *Psidium guajava* (guava) and *Azadirachta indica* (Neem) leaves with a ratio of 1:1 was weighed and washed before being air dried for 4-5 hours at room temperature. Weighed leaves were cut into small pieces and drenched in 150 ml of water overnight. The leaves mixture was then poured into 100 mL of de-ionized water, boiled, and stirred on a hot plate for 25-30 minutes at 80-90°C to ensure complete isolation. The mixture turned yellow on heating at a high temperature which showed the successful formation of extract. The extract was filtered after cooling and then placed at 4 °C in a refrigerator with proper labeling. A 0.2 M Zn (NO<sub>3</sub>)<sub>2</sub> .6H<sub>2</sub>O solution was prepared and heated at 60-70 °C on a hot plate followed by dropwise addition of 50 ml of 10% leaf extract. This led to the settlement of bio-reduced salt at the bottom of the flask which appeared as a white precipitate. Since the pH of the blend was slightly acidic (4.53), it was changed to 12 with a 0.4 M sodium hydroxide solution. The mixture was then heated for 10-15 minutes on a hot plate magnetic stirrer at 60-65 °C with intense stirring followed by sonication in an ultrasonic bath containing 1L deionized water 0.1% (w/w) of the sample, central position on the bottom of the tank for an hour. After ultra-sonication, the mixture is in the form of a transparent suspension. The powdered material Zn (OH)<sub>2</sub> was then oven dried for 3 hours at 60-70 °C and was fully converted to dark yellow-colored ZnO. This paste was placed in a porcelain crucible and calcined for 2 hours at 400 °C. After calcination, the ZnO was ground into a fine powder and stored.

### Characterization of ZnO NPs

The prepared ZnO NPs were analyzed using SEM analysis and Fourier transform infrared (FTIR) techniques as mentioned below.

### SEM and FTIR analysis of ZnO NPs

A scanning electron microscope was used to study the surface morphology particle size analysis of the ZnO NPs using NOVA-NANOSEM-450. ZnO NPs were mounted on aluminum stumps and protected with double-sided glue friction tape. Finally, the specimens were perceived using a 5 KV increasing voltage and an 11 mm operational space. FT-IR spectroscopy was used to examine the functionalities associated with ZnO NPs. The FT-IR spectrum was recorded using Cary-630 FT-IR Spectrometer at wavelengths ranging from 400 to 4000 cm<sup>-1</sup> at a resolving power of 4 cm<sup>-1</sup>. Data examination of each film has been executed through the FTIR Spectrum Software.

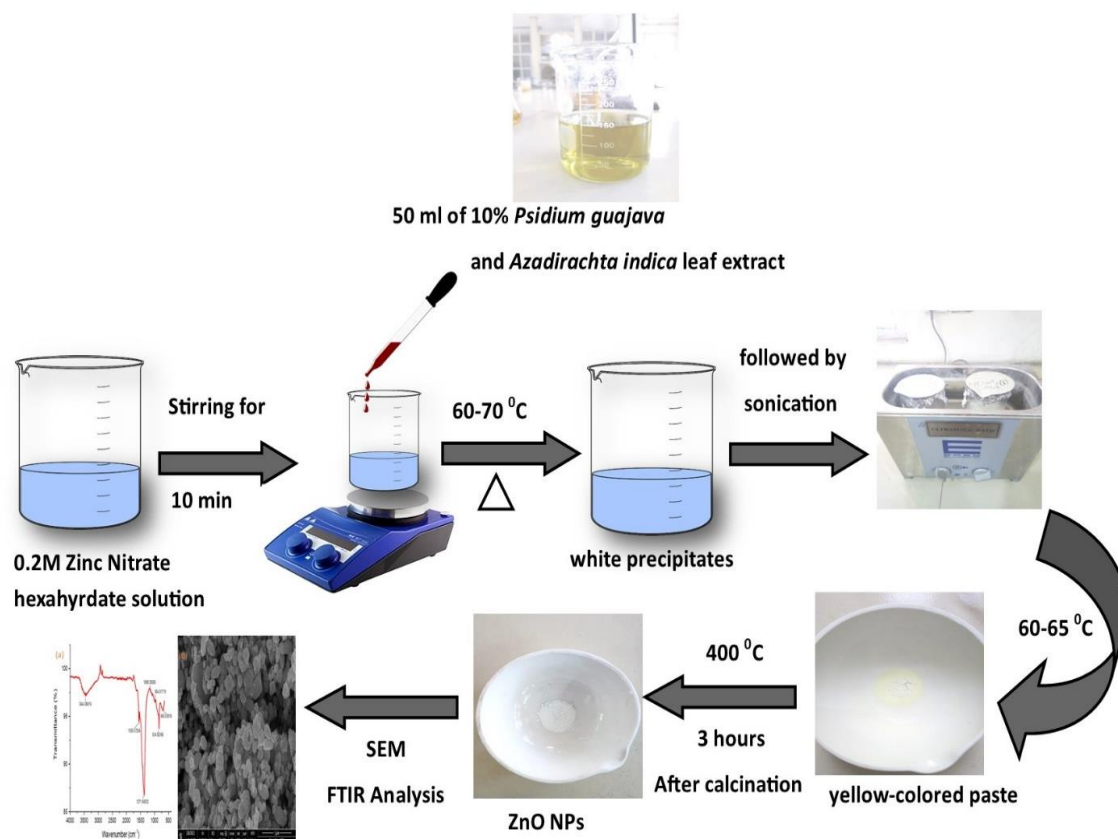


Fig. 1: Schematic representation of ZnO NPs synthesized from *Psidium guajava* and *Azadirachta indica* leaf extracts.

*Fabrication of starch bioplastic and composite bioplastic* (0.05 g / 5 g starch), 3%, (0.15 g / 5 g starch), 5 % (0.25 g / 5 g starch), 7 % (0.35 g / 5 g starch), and 10 % (0.5 g / 5 g starch).

The biodegradable starch and composite plastic films were fabricated using the solution casting method [30]. Starch bioplastic was fabricated by taking 5g of sweet potato starch in a beaker followed by the addition of 2 ml (40% of the weight of starch) of glycerol, 0.5ml of vinegar to adjust the pH of starch, and 60 ml of di-ionized water into the beaker.

The blend was mixed on a hot plate magnetic stirrer with the temperature gradually rising to 70 °C for 40-45 minutes and the pH of the resulting plastic solution was checked with a pH meter. The mixture was cooled to about 25 °C and cast into the petri dish, dried in an oven for 12 hours at 60 °C, and followed by cooling in a desiccator for 4-5 days. The simple starch bioplastic films thus obtained were stored in airtight plastic bags at room temperature. ZnO incorporated bioplastic nanocomposite films were also prepared by the above-mentioned method, with water being substituted by the ZnO NPs solution in water during sonication. ZnO composites were prepared using different concentrations of ZnO NPs i.e., 1%

*Characterization of starch and composite bioplastic films*

*Mechanical properties and Water vapor permeability (WVP)*

Mechanical properties of composite bioplastic films such as tensile strength and percentage of elongation at the break were determined by a TA XT Plus Texture Analyzer. Film samples were evaluated with some modifications and the tests were conducted according to the ASTM D828–97 standard test methods (ASTM, 1997). ZnO nanoparticle composite films were cut into strips (16×10 cm). The clamp distance was 20 mm, and the draw rate was 100 mm/min. Tensile strength was calculated by dividing the maximum load by the cross-sectional area of the film. The percentage of elongation at the break was expressed as a percentage of change of the original length of a specimen between grips at the break. Before the testing, the samples were preconditioned at

67% RH for 48 h at room temperature ( $25 \pm 1^\circ\text{C}$ ). All samples were collected in triplicate.

Before the Water vapor permeability (WVP) testing, the films were conditioned at  $25^\circ\text{C}$  for 48 h in a desiccator with a relative humidity of 65%. Circular film samples were put over the mouth of the test cup and wrapped with melted paraffin in the desiccator. The test cup was about 10 mm in diameter. Anhydrous calcium chloride (0% RH) was placed inside the test cup while a saturated sodium chloride solution (75% RH) was placed in the desiccator. The change in the weight of the cups was assessed every 12 h over two days. The gravimetric method was employed to find out the WVP of starch and composite bioplastic films. The WVP was determined as follows:

$$WVP = m \times d / (A \times t \times P) \quad (1)$$

where  $d$  is film thickness (m),  $m$  is the weight increment of the cup (g),  $A$  is the area exposed ( $\text{m}^2$ ),  $t$  is the time lag for permeation (h), and  $P$  is water vapor partial pressure difference across the film (Pa). All samples were carried out in triplicate. The thickness of the composite bioplastic films ( $t$ ) in mm was determined by using an electronic micrometer (Micro-master<sup>®</sup>) that was accurate to about 0.001 mm according to the method mentioned in the literature [31].

#### *SEM Analysis of Bioplastic Films*

A scanning electron microscope was used to assess the micro-structural analysis of the composite bioplastic (NOVA-NANOSEM-450) by the same method as described above.

#### *Functional group Analysis through FT-IR*

Functional classes of starch bioplastic and composite bioplastic films were revealed from FTIR spectrums recorded at wavelengths ranging from 400 to  $4000 \text{ cm}^{-1}$  using a Cary-630 FT-IR Spectrophotometer.

#### *UV Absorbance and transparency of bioplastic films*

The UV absorption and transparency of the bioplastic samples were measured using an Agilent-60 UV-visible spectrophotometer according to the procedure mentioned in the literature [32] with minor adjustments. To balance the height and width of the cuvette, the bioplastic was cut to  $1 \text{ cm} \times 3.5 \text{ cm}$ . Bioplastic composites were then put in the cuvette's crosswise direction and absorbance was recorded between 750 nm and 200 nm [33]. The UV absorbance of composite bioplastic films was determined by

dividing the maximum absorbance at a given wavelength (600 nm) by the thickness of the bioplastic film. The transmittance was calculated by using the equation below.

$$\%T = \text{antilog} (2 - \text{Absorbance}) \quad (2)$$

Where, %T = Transmittance at 600nm

The transparency of films was calculated using the equation,

$$\text{Transparency} = \frac{\log \%T}{b} \quad (3)$$

where,  $b$  = Thickness of bioplastic (mm)

Conventional polyethylene plastic bag was used as a reference.

#### *TGA studies*

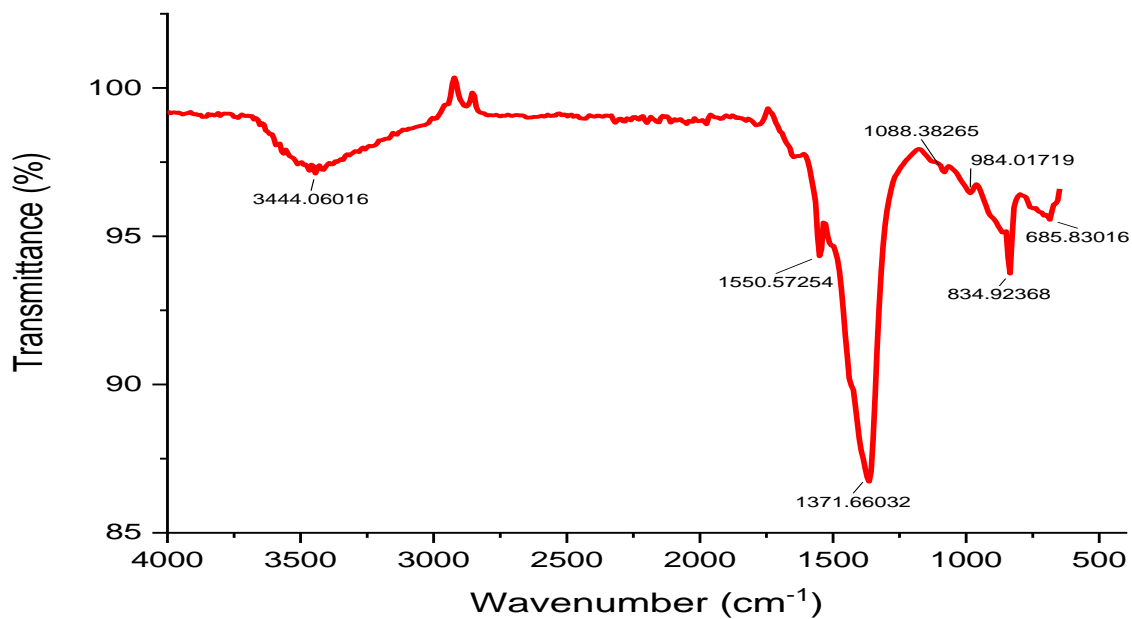
TGA of bioplastics was performed with TGA- Instrument TGA-50. The mass of the starch bioplastic and composite bioplastics were 13.286 and 9.778 mg respectively, and the temperature was increased by  $10^\circ\text{C}$  per min, starting at  $30^\circ\text{C}$  and increasing to  $500^\circ\text{C}$ , using aluminum cell in  $\text{N}_2$  atmosphere with a flow rate of 30 ml/min. The TGA graphs were evaluated to reveal the onset, peak, and end temperatures, and the weight loss changes of biocomposite films.

#### *DSC Analysis*

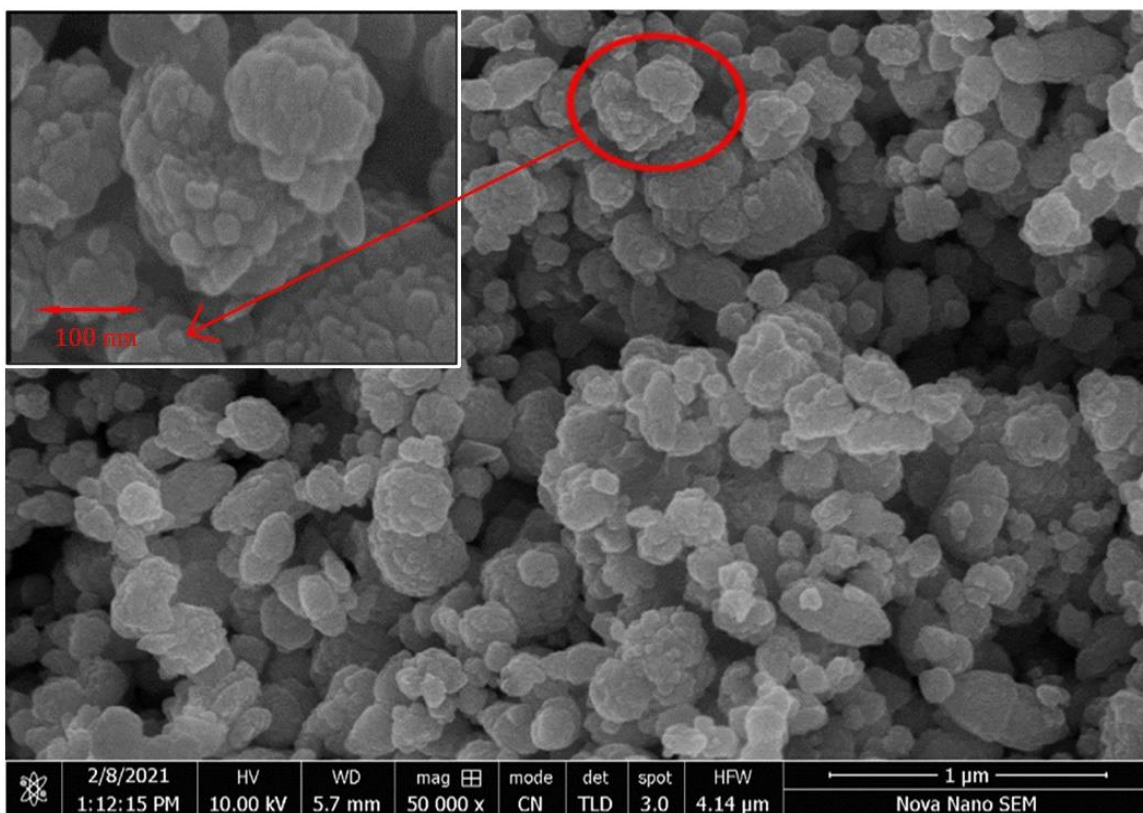
DSC analysis of the bioplastics was performed using a DSC-60A instrument in an aluminum cell under  $\text{N}_2$  atmosphere using a sample weight of 6 mg for starch bioplastic and 5.2 mg for composite bioplastic. The temperature was increased by  $10^\circ\text{C}$  per min beginning from  $30^\circ\text{C}$  up to  $400^\circ\text{C}$  with a flow rate of  $\text{N}_2$  gas of about 45 ml/min. The heat flow rate profile was measured as a function of temperature. The DSC thermograms were assessed to indicate the onset, peak, and end temperatures, and the enthalpy changes of the phase transitions.

#### *Soil burial decomposition analysis*

In the laboratory, biodegradation tests of bioplastic films were carried out using the method suggested in the literature [34] with some minor modifications. Starch bioplastic and composite films with dimensions of  $60 \text{ mm} \times 30 \text{ mm} \times 2 \text{ mm}$  were buried at a depth of 20 cm in the soil.



(a)



(b)

Fig. 2: (a) FT-IR spectrum (b) SEM images of ZnO NPs synthesized from guava and neem leaf extracts.

Table-1: Water vapor permeability (WVP) and Physical properties of starch and composite bioplastic films.

Physical Appearance	ZnO NP reinforced composite bioplastic					
	0%	1%	3%	5%	7%	10%
Texture	Smooth surface and less flexible	Smooth Surface	Slightly rough and elastic	Highly Even	Smooth surface	Flexible with a smooth surface
Brittleness	High	High	Moderate	Moderate	High	Moderate
Surface	Transparent	Transparent	Transparent	Transparent	Highly Transparent	Highly transparent
Film thickness (mm)	0.12	0.28	0.27	0.38	0.28	0.01
WVP ( $10^{-10} \text{ g Pa}^{-1} \text{ s}^{-1} \text{ m}^{-1}$ )	5.36	3.79	2.98	1.58	2.32	2.65

The soil was kept in the research lab using a plastic container, and the soil's humidity was maintained by watering after various periods i.e., 15, 30, and 60 days. Synthetic polyethylene plastic was utilized as a reference and mass loss of the sample over time was used to determine the decomposition rate of the soil burial test. The following equation was employed to calculate the biodegradation mass loss after a 15-day break.

$$\text{Mass loss \%} = \frac{M_1 - M_2}{M_1} \times 100\% \quad (4)$$

Where,

$M_1$  = Initial mass

$M_2$  = Final mass of the sample after drying

## Results and Discussion

### Characterization of ZnO NPs

The presence of several functional groups in green synthesized ZnO NPs was examined using the FT-IR spectrum [35]. Fig. 2 (a) displays the FTIR spectrum of ZnO NPs synthesized from guava and neem leaf extracts. The metal oxide peak appeared at a wavenumber less than  $1000 \text{ cm}^{-1}$  in the fingerprint region of the spectrum. The deformation of the ZnO bond has been indicated in the form of a sharp band at  $834 \text{ cm}^{-1}$ , while the stretching can be seen in a peak at  $1550 \text{ cm}^{-1}$ . The morphology and surface structure of ZnO NPs was examined using SEM. Fig. 2 (b) shows the SEM image of ZnO NPs at a particular resolution. The SEM photograph revealed the spherical shape of NPs with diameters ranging between 80-100 nm. Accumulated ZnO NPs and the individual NPs exhibited relatively smaller sizes in the range of 20-100 nm. A similar structure was reported in some studies when an aqueous extract from *Azadirachta Indica* was used [36].

### Characterization of the starch and composite bioplastic films

#### Mechanical properties and Water vapor permeability (WVP)

The water vapor permeability (WVP) of starch and composite bioplastic films is shown in

Table-1. WVP of the films is important when it is used as packaging material. In such cases one of the functions of the film is to avoid, or at least to decrease, moisture transfer between the food and the surrounding atmosphere; WVP should be as low as possible. As can be seen from Table-1, the pure bioplastic films had the highest WVP ( $5.36610210 \text{ g Pa}^{-1} \text{ s}^{-1} \text{ m}^{-1}$ ), which was significantly higher than starch composite films containing ZnO nanoparticles. When the content of ZnO NPs was 5%, the blend films had the lowest value of WVP. The enhancement in water vapor resistance with the addition of ZnO NPs can be due to their nanometric size, which increases the surface volume ratio and promotes a better dispersion of the nanoparticles in the starch matrix. The well-distributed nanoparticles can generate a curved path and force water molecules to flow through the composite in a tortuous path, decreasing their diffusion through the film. In addition, the ZnO NPs are less hydrophilic than starch, making the film more hydrophobic. It had been previously acknowledged that the nanoparticles could prevent the formation of hydrogen bonding between starch molecules, giving rise to a more compact structure with smaller inter-chain spaces that can reduce the water vapor diffusion through the film. In general, ZnO NPs composite films showed better barriers to water vapor.

The effect of ZnO NPs content on mechanical properties is presented in Table-2. Food packaging usually demands resistance to high stress with deformation according to the proposed applications. The pure bioplastic films had the lowest mechanical properties. The addition of ZnO NPs significantly improved tensile strength, elongation at the break, and Young's modulus, which increased from 1.41 to 2.26 MPa, 78.20 to 114.91%, and 1.62 to 2.40 MPa, respectively. The tensile strength of the films increased with the addition of ZnO NPs content up to 5% and then decreased as the increase of the nanoparticle content went on. It appeared as if loading more than 5% of the nanoparticles did not lead to a greater effect because of the phase separation between the nanoparticle aggregates and starch matrix. The increased mechanical properties might be attributed to the good dispersion state of nanoparticles and the

interactions between ZnO NPs and chain segments of bioplastic starch, which reduced chain mobility and hence improved the macroscopic rigidity of ZnO NPs composite films. Further, it is reported that nanocomposites exhibited a remarkable improvement in the mechanical properties, especially in the Young's modulus and this was due to the filler surface-polymer chain segments interactions which reduced chain mobility and hence improved macroscopic rigidity. Nanofillers act efficiently as matrix reinforcement, but only if they are well dispersed, so the interface with the matrix would be extended. Film thickness reveals crucial details about the structure of bioplastics and was also used to calculate the transparency of bioplastic films. The thickness of the films varied from 0.01 to 0.38 mm which decreased with an increase in the concentration of NPs by the values mentioned in the literature [37]. All the physical characteristics related to the structure of the starch bioplastic film and composite bioplastic films made were analyzed and presented in Table-1.

#### SEM Analysis of Bioplastic Films

Fig. 3(a) demonstrates the SEM micrographs of starch bioplastic comprised of particles representing that the starch has not been entirely gelatinized through the materialization procedure. Furthermore, composite bioplastic's open-to-air exteriors are

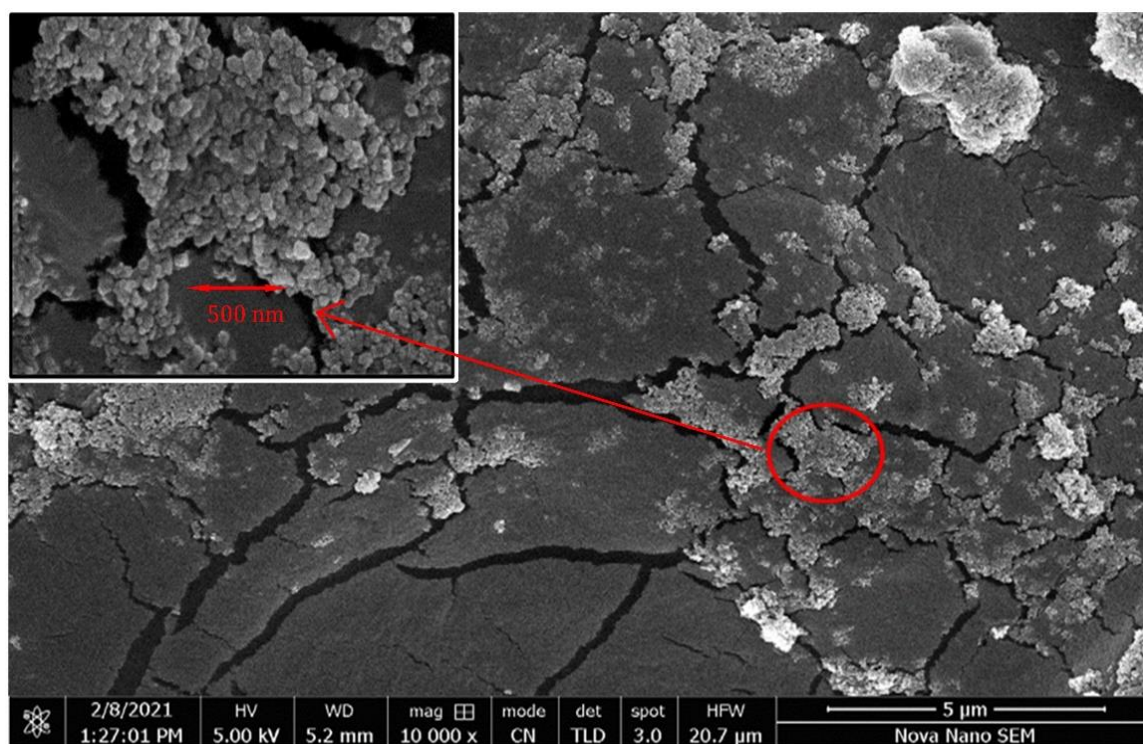
abnormal with channels and show appearance of non-gelatinized ZnO NPs. The surface structure presents few gaps which had no or little effect on mechanical properties of biocomposite and reduced interfacial linkage indicating a lower level of attachment between the constituents as shown in Fig. 3(b).

Hence, starch bioplastic had a stable and even surface due to the small amount of residual starch particles and the absence of non-gelatinized ZnO compared to composite bioplastics. The presence of ZnO NPs increased the surface unevenness of the starch bioplastic and decreased its consistency.

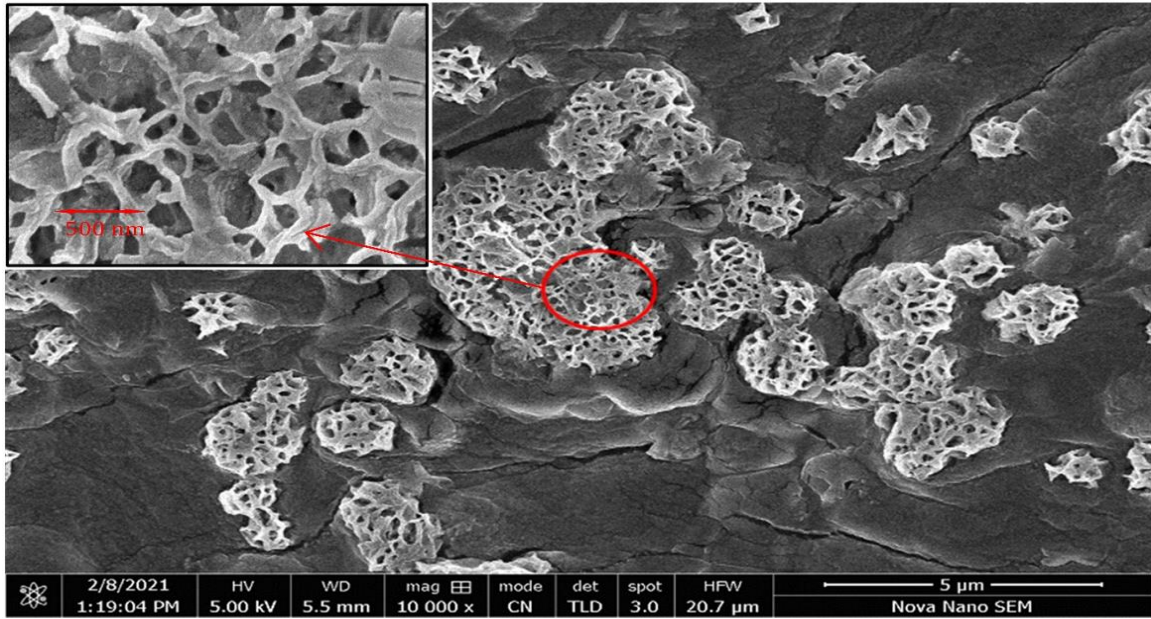
#### FT-IR analysis of composite bioplastic

Fig. 4(a) and 4(b) show FTIR analysis of a bioplastic film made from starch and 5 % ZnO NPs giving highly even texture. The presence of -C-O-H, -O-H, -C-H aliphatic, and -C=O groups in bioplastics were confirmed according to Fourier transform infrared spectra.

The interaction between the biopolymer matrix and the NPs is confirmed by the significant change in peaks between  $849.7\text{ cm}^{-1}$  and  $872.3\text{ cm}^{-1}$  and the highest values of the polymer matrix shift occur at  $849.8\text{ cm}^{-1}$ .

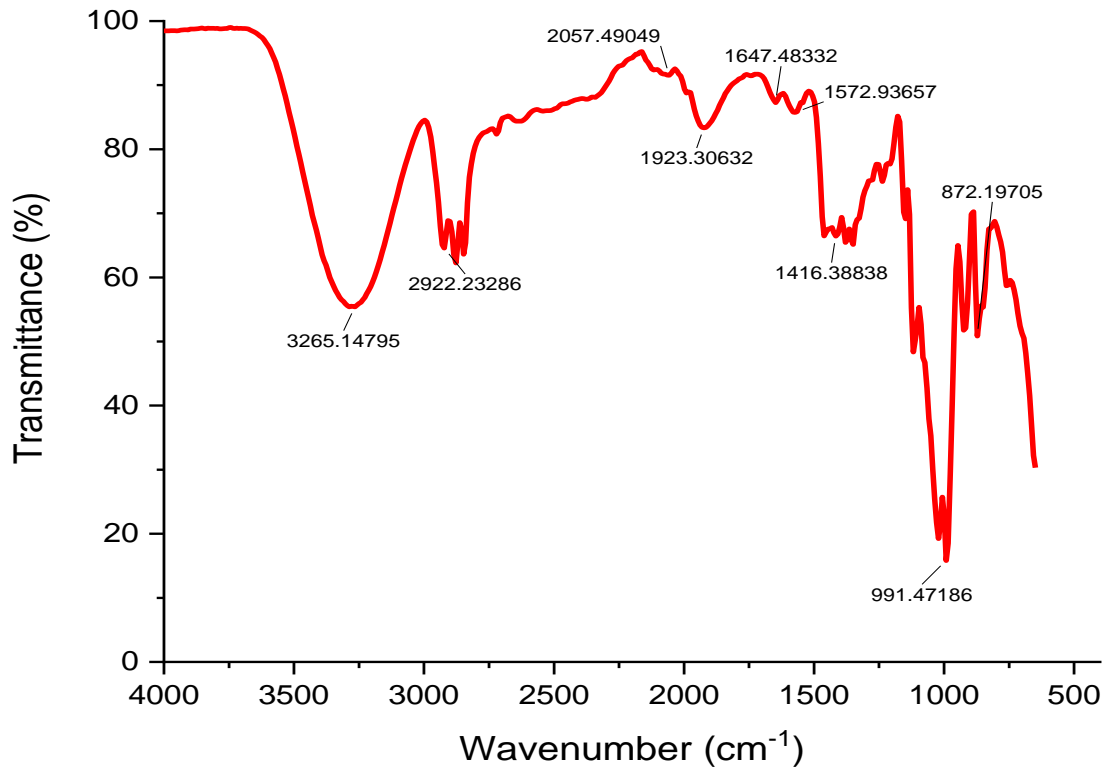


(a)

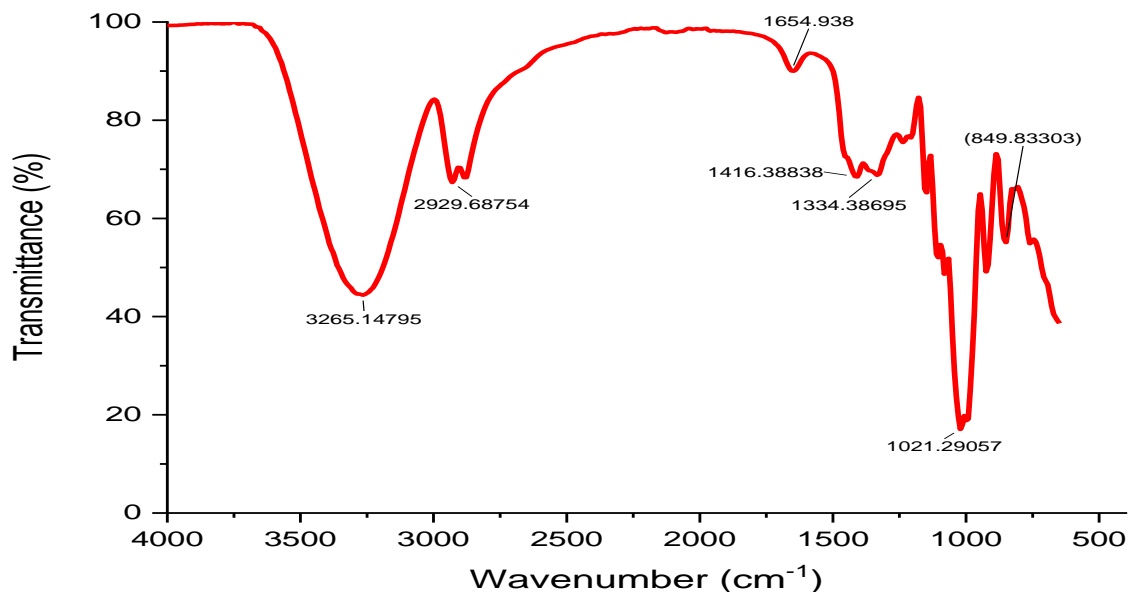


(b)

Fig. 3: SEM micrographs of (a) starch bioplastic 10000X 5μm and (b) composite bioplastic 10000X 5μm prepared by using 5% ZnO NPs.



(a)



(b)

Fig. 4: (a) FT-IR spectrum of simple starch bioplastic film (b) FT-IR spectrum of 5% ZnO NPs reinforced composite bioplastic films.

Table-2: Mechanical properties of starch bioplastic and composite bioplastic films.

ZnO NPs composite bioplastic films (Type %)	Tensile strength/MPa	Elongation at break/%	Young's modulus/MPa
0% (Starch bioplastic)	1.41	78.20	1.62
1%	1.86	107.67	1.97
3%	1.94	113.32	2.13
5%	2.26	114.91	2.40
7%	1.93	108.91	1.92
10%	1.83	105.57	1.84

Table-3: FT-IR data of the starch bioplastic and composite bioplastic.

Types of vibrations	Peak Values (cm <sup>-1</sup> ) For ZnO NPs Incorporated Composite Bioplastic					
	0%	1%	3%	5%	7%	10%
O-H Stretching	3265.1	3265.1	3265	3265	3265.1	3265.1
Zn-O bond Deformation	-	849.8	849.7	872.3	849.8	849.8
C-H Stretching linked to H-atoms	2929.3	2929.7	2929.1	2922.2	2937.1	2929.7
Symmetric and Asymmetric – COOH vibrations	1416.4	1416.4	1654.9	1416.4	1416.1	1416.4
	1654.9	1654.9	1565.5	1647.5	1647.6	1654.9
-C-O Stretching of C-O-H group	1334.4	1334.3	1410.4	1150.3	1341.8	1341.8
-C-O Stretching of C-O-C group	1021.3	1013.8	1021.3	991.5	1021.3	998.9
	849.8					

The electrostatic attraction between ZnO NPs and the hydroxyl groups of the polymer matrix is responsible for the change in (i) C-H stretching of methyl and methylene groups from 2929.7 cm<sup>-1</sup> (in the case of starch bioplastic) to the lower absorption band 2937.1 cm<sup>-1</sup> (in the presence of 5% ZnO NPs in case of composite bioplastic) (ii) C-O bond stretching of the C-O-C- group of the simple starch composite from 1021 cm<sup>-1</sup> -1013 cm<sup>-1</sup> to 998-991 cm<sup>-1</sup> in the presence of 10% ZnO composite. Polymer-nanoparticle interaction is evident from the regular shifts in the

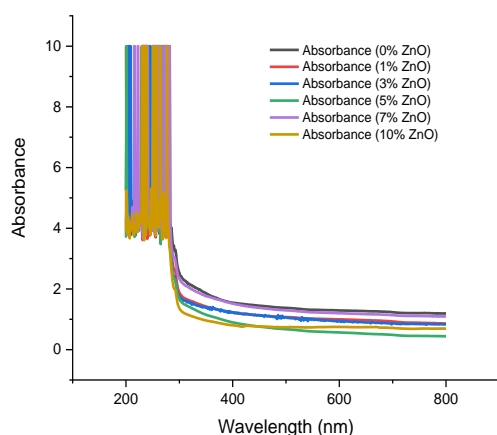
absorption peaks with subsequent ZnO incorporation. All the peaks acquired were referred to the prior literature [38] for confirmation and presented in the tabular form Table-3.

#### UV Absorption and transparency of starch and composite bioplastics

The bioplastic is capable of shielding food products from UV rays and avoiding photo-oxidative decomposition which would alter the odor and

contribute to the creation of free radicals [39]. Additionally, the free radicals produce lipid rancidity and DNA transformations that trigger various illnesses like skin cancer, damaged nervous system, and coronary heart disease.

Fig. 5 displays the UV spectrum of starch bioplastic and ZnO NPs incorporated composite bioplastic with the maximum absorption in the wavelength range from 200 nm to 400 nm. The greater the amount of ZnO NPs in the bioplastic, the greater the bioplastic's ability to absorb UV radiation. The bioplastic containing 5% ZnO NPs exhibited maximum absorbance at 600 nm and 10% ZnO NPs at 200-400 nm. The transparency of the bioplastic was examined by measuring the transmitted light at 600 nm to obtain numerical results using a spectrophotometer.



(a)

Fig. 5: UV spectrum of starch bioplastic and ZnO NPs incorporated composite bioplastic films.

Table-4. showed that bioplastic was transparent, and the composite bioplastic film reinforced with 10% ZnO NPs exhibited higher transparency compared to other composites. The transparency of bioplastic was calculated using the percentage transmittance by equation (2). Transparency values displayed by the composite bioplastic appeared relatively intermediary to the simple bioplastic film.

#### Thermo-gravimetric Analysis (TGA)

Fig. 6 demonstrates the curves of starch bioplastic and composite bioplastic respectively acquired through thermo-gravimetric analysis. The

primary breakdown of the starch bioplastic film sample occurred at 172.60 °C implied by the reduction in specimen mass followed by single phase breakdown up to 333.62 °C, losing about half of its mass. It is revealed that the breakdown of both starch bioplastic and composite occurred in two steps (1) the moisture confined in starch bioplastic is evaporated along with vinegar removal (60–210 °C) and (2) thermal breakdown of starch bioplastic (220-339 °C) and composite bioplastic (at 339.60 °C between 240-410 °C) occurred along with vaporization of glycerol (249.48-333.62 °C). The fragmentation data of starch bioplastic and composite bioplastic showed that 50 percent of mass loss occurred at 276.56 °C and 275.13 °C for starch bioplastic and composite bioplastics, respectively.

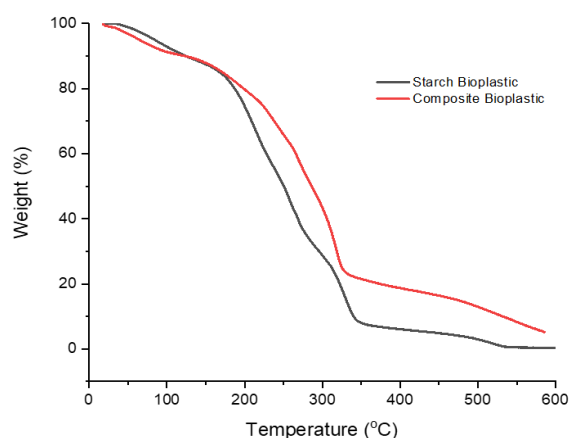


Fig. 6: Thermogravimetric analysis (TGA) curve for starch bioplastic and 5% ZnO NPs reinforced composite bioplastic.

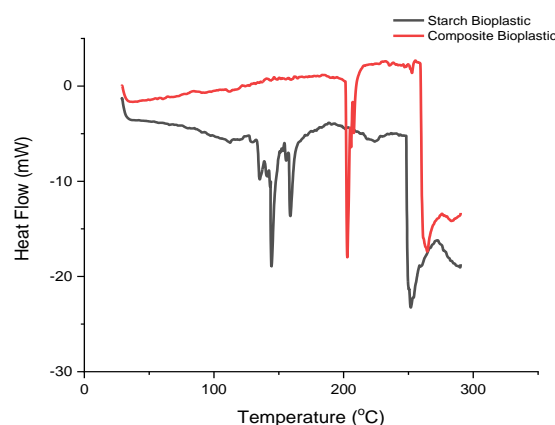


Fig. 7: Differential Scanning Calorimetry (DSC) thermo-gram of starch bioplastic and 5% ZnO NPs incorporated composite bioplastic.

Within the range of 33.14°C–500 °C, the overall results of the physical and thermal characteristics investigation of the bioplastic indicate that the key reduction in mass is -99.416 % and -99.616 % with 5% ZnO incorporated composite bioplastic and starch bioplastic, respectively. The addition of ZnO NPs to bioplastic raises the breakdown temperature leading to the improved heat stability of composite bioplastics.

#### Differential Scanning Calorimetry (DSC) analysis

Starch and composite bioplastics are found to have the highest melting temperatures of 144.44 °C and 201.86 °C, respectively, as presented in Fig. 7. It has been reported that the melting point of the films has increased radically by the presence of NPs[40] due to intensification in the degree of nanocomposite crystallinity and interfacial interaction between the NPs and the amorphous region of the chain.

The Starch Bioplastic has a semi-crystalline structure having a crystallization temperature of 147 °C and exhibiting two contemporary peaks between 260 °C and 340 °C in the DSC curve. The glass transition temperature ( $T_g$ ) of starch bioplastic and bioplastic composite films is found to be the same, nearly 76.5 °C, as calculated by the results of DSC levels. The higher the glass transition temperature of a polymer, the better its resistance properties.

Consequently, glass transition temperature ( $T_g$ ) specifies the uniformity of the constituents with biopolymer. ZnO NPs can make chemical bonds with O-H of the starch molecules. Therefore, the results indicate the higher thermal stability for the starch and ZnO NPs reinforced composite bioplastic films.

#### Soil burial biodegradation test

The soil submerged bioplastic samples were removed from the soil at different time intervals for soil biodegradation analysis. It was found that the color and mass of bioplastic films began to exhibit slight change on day 15.

Fig. 8 represents the appearance and percentage of mass loss of bioplastic films after soil burial. The highest percentage of mass loss was observed as 85 % and 74 % for starch and composite bioplastic respectively after 30 days of soil burial while no difference in polyethylene occurs. Starch-based films, both with and without NPs, have already been reported that disintegrate completely within 60 days [41]. So, compared to traditional plastics, starch bioplastic composites have the potential to decompose quickly, and all the plastics manufactured in this study decomposed easily and hence can be called decomposable products.



Fig. 8: Biodegradation of (a) starch bioplastic, (b) 5% ZnO NPs reinforced composite bioplastic, and (c) polyethylene plastic.

Table-4: UV absorption and transparency analysis of starch bioplastic and composite bioplastic films

ZnO NPs composite bioplastic films (Type %)	Absorbance	Transmittance (%)	Thickness (mm)	Transparency
0% (starch bioplastic)	4.317	0.098	0.12	0.08
1%	4.129	0.118	0.28	0.37
3%	4.332	0.097	0.27	0.44
5%	4.469	0.084	0.38	0.65
7%	4.336	0.096	0.25	0.41
10%	3.781	0.168	0.01	1.22
Polyethylene film	5.3	0.03	0.01	0.47

## Conclusion

This investigation was conducted to produce biodegradable and economical bioplastic from plant sources. Bioplastics were developed using sweet potato starch with and without reinforcement with biogenically synthesized ZnO NPs. These bioplastics have impressive decomposable properties as well as strong interfacial bonding and thermal properties rendering them a viable alternative to existing traditional plastics. Furthermore, starch is a low-cost, renewable resource. The durable interaction between polymer matrix and ZnO NPs confirmed the formation of bio nanocomposite through FT-IR analysis. It was observed that the ZnO NPs had significant effects on the tensile properties of the nanocomposite films. The addition of ZnO NPs to the starch bioplastic films substantially improved tensile strength, elongation, and Young's modulus. The integration of ZnO NPs lowered the degree of WVP and film solubility value contrasted to those of the CS films. The thermal stability and transparency of the prepared bioplastic are increased by the addition of ZnO NPs for its application in the packaging industry. Biodegradation of these bioplastic films under natural conditions has proven that the composite bioplastic is compostable (85%) according to the international standards of bioplastic disintegration EN13432. Hence, it is concluded that the prepared composite bioplastic from renewable resources provides UV protection, mechanical strength, thermal stability, and biodegradability.

## Declaration of Interest

We declare that this manuscript is original, has not been published before and is not currently being considered for publication anywhere. We confirm that the manuscript has been read and approved by all named authors and that there are no other people who satisfied the criteria for authorship but are not listed. We further confirm that the order of authors listed in the manuscript has been approved by all of us.

We understand that the Corresponding Author is the sole contact for the Editorial process. She is responsible for communicating with the other authors about progress, submissions of revisions and final approval of proofs.

## References

1. K. Chidambarampadmavathy, O. P. Karthikeyan, and K. Heimann, Sustainable bio-plastic production through landfill methane recycling, *Renewable and Sustainable Energy Reviews.*, **71**, 555 (2017).
2. R. Sharma, S. M. Jafari, and S. Sharma, Antimicrobial bio-nanocomposites and their potential applications in food packaging, *Food Control.*, **112**, 107086 (2020).
3. M. Barletta and M. Puopolo, *J. Manuf. Process* Thermoforming of compostable PLA/PBS blends reinforced with highly hygroscopic calcium carbonate, *J. Manufacturing Proc.*, **56**, 1185 (2020).
4. T. N. Tran, B. T. Mai, C. Setti, and A. Athanassiou, Transparent Bioplastic Derived from CO<sub>2</sub>-Based Polymer Functionalized with Oregano Waste Extract toward Active Food Packaging, *ACS Appl. Mater. Interfaces.*, **12**, 46667 (2020).
5. D. Adhikari, M. Mukai, K. Kubota, T. Kai, N. Kaneko, K. S. Araki, and M. Kubo, Degradation of Bioplastics in Soil and Their Degradation Effects on Environmental Microorganisms, *J. Agric Chem. Environ.*, **05**, 23 (2016).
6. S. K. Bhatia, R. Gurav, T. R. Choi, H. R. Jung, S. Y. Yang, Y. M. Moon, H. S. Song, J. M. Jeon, K. Y. Choi, and Y. H. Yang, Bioconversion of plant biomass hydrolysate into bioplastic (polyhydroxyalkanoates) using *Ralstonia eutropha* 5119, *Bioresour. Technol.*, **271**, 306 (2019).
7. T. Bhuyan, K. Mishra, M. Khanuja, R. Prasad, and A. Varma, Biosynthesis of zinc oxide nanoparticles from *Azadirachta indica* for antibacterial and photocatalytic applications, *Mater. Sci. Semicond. Process.*, **32**, 55 (2015).

8. M. I. Din, R. Sehar, Z. Hussain, R. Khalid, and A. T. Shah, Synthesis of biodegradable semolina starch plastic films reinforced with biogenically synthesized ZnO nanoparticles, *Inorg. Nano-Metal Chem.*, **51**, 985 (2021).
9. R. F. Santana, R. C. F. Bonomo, O. R. R. Gandolfi, L. B. Rodrigues, L. S. Santos, A. C. dos Santos Pires, C. P. de Oliveira, R. da Costa Ilhéu Fontan, and C. M. Veloso, Characterization of starch-based bioplastics from jackfruit seed plasticized with glycerol, *J. Food Sci. Technol.*, **55**, 278 (2018).
10. J. Yang, Y. C. Ching, C. H. Chuah, N. D. Hai, R. Singh, and A. R. M. Nor, Preparation and characterization of starch-based bioplastic composites with treated oil palm empty fruit bunch fibers and citric acid, *Cellulose.*, **28**, 4191 (2021).
11. N. Méité, L. K. Konan, M. T. Tognonvi, B. I. H. G. Doubi, M. Gomina, and S. Oyetola, Properties of hydric and biodegradability of cassava starch-based bioplastics reinforced with thermally modified kaolin, *Carbohydr. Polym.*, **254**, 117322 (2021).
12. K. Martinez Villadiego, M. J. Arias Tapia, J. Useche, Y. Ledesma, and A. Leyton, Thermal and Morphological Characterization of Native and Plasticized Starches of Sweet Potato (*Ipomoea batatas*) and Diamante Yam (*Dioscorea rotundata*), *J. Polym. Environ.*, **29**, 871 (2021).
13. N. Nordin, S. H. Othman, S. A. Rashid, and R. K. Basha, Effects of glycerol and thymol on physical, mechanical, and thermal properties of corn starch films, *Food Hydrocoll.*, **016**, 105884 (2020).
14. A. H. Mohsen and N. A. Ali, Mechanical, Color and Barrier, Properties of Biodegradable Nanocomposites Poly(lactic Acid)/Nanoclay, *J. Bioremediation Biodegrad.*, **09**, 1 (2018).
15. A. H. D. Abdullah, O. D. Putri, A. K. Fikriyyah, R. C. Nissa, S. Hidayat, R. F. Septiyanto, M. Karina, and R. Satoto, Harnessing the Excellent Mechanical, Barrier and Antimicrobial Properties of Zinc Oxide (ZnO) to Improve the Performance of Starch-based Bioplastic, *Polym. Technol. Mater.*, **59**, 1259 (2020).
16. F. Luzi, L. Torre, M. Kenny, and D. Puglia, Bio- and Fossil-Based Polymeric Blends and Nanocomposites for Packaging: Structure–Property Relationship, *Materials (Basel)*, **12**, 1 (2019).
17. P. Jariyasakoolroj, P. Leelaphiwat, and N. Harnkarnsujarit, Advances in research and development of bioplastic for food packaging, *J. Sci. Food Agric.*, **100**, 5032 (2020).
18. M. I. Din, J. Najeeb, Z. Hussain, R. Khalid, and G. Ahmad, Biogenic scale up synthesis of ZnO nano-flowers with superior nano-photocatalytic performance, *Inorg. Nano-Metal Chem.*, **50**, 613 (2020).
19. H. Yue, Y. Zheng, P. Zheng, J. Guo, J. P. Fernández-Blázquez, J. H. Clark, and Y. Cui On the improvement of properties of bioplastic composites derived from wasted cottonseed protein by rational cross-linking and natural fiber reinforcement, *Green Chem.*, **22**, 8642 (2020).
20. G. Mannina, D. Presti, G. Montiel-Jarillo, and M. E. Suárez-Ojeda, Bioplastic recovery from wastewater: A new protocol for polyhydroxyalkanoates (PHA) extraction from mixed microbial cultures, *Bioresour. Technol.*, **282**, 361 (2019).
21. S. A. Oleyaei, Y. Zahedi, B. Ghanbarzadeh, and A. A. Moayedi, Modification of physicochemical and thermal properties of starch films by incorporation of TiO<sub>2</sub> nanoparticles, *Int. J. Biol. Macromol.*, **89**, 256 (2016).
22. P. Kanmani and J. W. Rhim, Properties and characterization of bionanocomposite films prepared with various biopolymers and ZnO nanoparticles, *Carbohydr. Polym.*, **106**, 190 (2014).
23. A. C. Jayasuriya, A. Aryaei, and A. H. Jayatissa, ZnO nanoparticles induced effects on nanomechanical behavior and cell viability of chitosan films, *Mater. Sci. Eng., C* **33**, 3688 (2013).
24. H. Wang, K. Xu, Y. Ma, Y. Liang, H. Zhang, and L. Chen, Impact of ultrasonication on the aggregation structure and physicochemical characteristics of sweet potato starch, *Ultrason. Sonochem.*, **63**, 1 (2020).
25. O. O. Oluwasina, B. P. Akinyele, S. J. Olusegun, O. O. Oluwasina, and N. D. S. Mohallem Evaluation of the effects of additives on the properties of starch-based bioplastic film, *SN Appl. Sci.*, **3**, 1 (2021).
26. A. M. Pillai., V. S. Sivasankarapillai., A. Rahdar., J. Joseph., F. Sadeghfar., K. Rajesh., & G. Z. Kyzas., Green synthesis and characterization of zinc oxide nanoparticles with antibacterial and antifungal activity. *J. Mole. Struc.*, **1211**, 128107 (2020).
27. A. Es-Haghi., M. E. Taghavizadeh Yazdi., M., M. Sharifalhoseini., M. Baghani., E. Yousefi., A. Rahdar., & F. Baino., Application of response surface methodology for optimizing the therapeutic activity of ZnO nanoparticles biosynthesized from *Aspergillus niger*. *Biomimetics.*, **34**, 6 (2021).
28. H. A. M. Wickramasinghe, S. Takigawa, C.

- Matsuura-Endo, H. Yamauchi, and T. Noda, Comparative analysis of starch properties of different root and tuber crops of Sri Lanka, *Food Chem.*, **112**, 98 (2009).
29. M. Naseer., U. Aslam., B. Khalid., & B. Chen., Green route to synthesize Zinc Oxide Nanoparticles using leaf extracts of Cassia fistula and Melia azadarach and their antibacterial potential. *Scientific Reports.*, **10**, 1 (2020).
30. A. Ostafińska, J. Mikešová, S. Krejčíková, M. Nevalová, A. Šturcová, A. Zhigunov, D. Micháľková, and M. Šlouf, Thermoplastic starch composites with TiO<sub>2</sub> particles: Preparation, morphology, rheology and mechanical properties, *Int. J. Biol. Macromol.*, **101**, 273 (2017).
31. C. E. F. Teixeira, I. de Almeida Rebechi, and R. S. Fontaneli, Digital Micrometer Used in Thickness Measurement of Plastic Film Compared to Standardized Instrument, *Mater. Sci. Appl.*, **08**, 577 (2017).
32. S. N. H. M. Azmin, N. A. binti M. Hayat, and M. S. M. Nor, Digital Micrometer Used in Thickness Measurement of Plastic Film Compared to Standardized Instrument, *J. Bioresour. Bioprod.*, **5**, 248 (2020).
33. F. Jia, J. J. Wang, Y. Huang, J. Zhao, Y. Hou, and S. Q. Hu, Development and characterization of gliadin-based bioplastic films enforced by cinnamaldehyde, *J. Cereal Sci.*, **99**, 103208 (2021).
34. E. C. Rada, G. Ionescu, N. Ferronato, M. Ragazzi, M. Raspanti, F. Conti, and V. Torretta, Zooming on light packaging waste differences by scanning electron microscopy, *Environ. Sci. Pollut., Res.*, **02**, 1 (2020).
35. M. C. Lavagnolo, F. Ruggero, A. Pivato, C. Boaretti, and A. Chiumenti, Composting of starch-based bioplastic bags: Small scale test of degradation and size reduction trend *Detritus.*, **12**, 57 (2020).
36. M. F. Sohail, M. Rehman, S. Z. Hussain, Z. e. Huma, G. Shahnaz, O. S. Qureshi, Q. Khalid, S. Mirza, I. Hussain, and T. J. Webster, Green synthesis of zinc oxide nanoparticles by Neem extract as multi-facet therapeutic agents, *J. Drug Deliv. Sci. Technol.*, **59**, 101911 (2020).
37. Q. Wang, J. Cai, L. Zhang, M. Xu, H. Cheng, C. C. Han, S. Kuga, J. Xiao, and R. Xiao, A bioplastic with high strength constructed from a cellulose hydrogel by changing the aggregated structure, *J. Mater. Chem., A* **1**, 6678 (2013).
38. K. Charoensri, C. Rodwihok, D. Wongratanaphisan, J. A. Ko, J. S. Chung, and H. J. Park, Investigation of functionalized surface charges of thermoplastic starch/zinc oxide nanocomposite films using polyaniline: The potential of improved antibacterial properties, *Polymers (Basel).*, **13**, 1 (2021).
39. I. Kim, K. Viswanathan, G. Kasi, S. Thanakkasaranee, K. Sadeghi, and J. Seo, ZnO Nanostructures in Active Antibacterial Food Packaging: Preparation Methods, Antimicrobial Mechanisms, Safety Issues, Prospects, and Challenges, *Food Rev. Int.*, **00**, 1 (2020).
40. M. R. Amin, M. A. Chowdhury, and M. A. Kowser, Characterization and performance analysis of composite bioplastics synthesized using titanium dioxide nanoparticles with corn starch, *Heliyon.*, **5**, e02009 (2019).
41. S. Jafarzadeh, A. Mohammadi Nafchi, A. Salehabadi, N. Oladzad-abbasabadi, and S. M. Jafari, Application of bio-nanocomposite films and edible coatings for extending the shelf life of fresh fruits and vegetables, *Advances in Colloid, and Interface Science.*, **291**, 102405 (2021).